

UC Irvine

UC Irvine Previously Published Works

Title

Tissue parameters determining the visual appearance of normal skin and port-wine stains

Permalink

<https://escholarship.org/uc/item/0j1692xj>

Journal

Lasers in Medical Science, 10(1)

ISSN

0268-8921

Authors

Svaasand, LO
Norvang, LT
Fiskerstrand, EJ
[et al.](#)

Publication Date

1995-03-01

DOI

10.1007/bf02133165

Copyright Information

This work is made available under the terms of a Creative Commons Attribution License, available at <https://creativecommons.org/licenses/by/4.0/>

Peer reviewed

Tissue Parameters Determining the Visual Appearance of Normal Skin and Port-wine Stains

L.O. SVAASAND^{a,b}, L.T. NORVANG^{a,b}, E.J. FISKERSTRAND^c, E.K.S. STOPPS^a,
M.W. BERNS^b, J.S. NELSON^b

^aNorwegian Institute of Technology, Division of Physical Electronics, University of Trondheim, N-7034 Trondheim, Norway

^bBeckman Laser Institute and Medical Clinic, 1002 Health Sciences Road East, University of California, Irvine, CA 92715, USA

^cDepartment of Dermatology, University Hospital, Trondheim, Norway

Correspondence to L. O. Svaasand, Norwegian Institute of Technology, Division of Physical Electronics, University of Trondheim, N-7034 Trondheim, Norway

Paper received 8 November 1994 and in revised form 30 May 1995

Abstract. Port-wine stain is a congenital birthmark consisting of an abnormal density of blood vessels in the upper dermis. The enlarged blood volume gives the lesion a red to purple colour. The aim of the treatments is to destroy the vessels to the extent necessary for obtaining a normal skin coloration. Thus, in principle, all relevant information about the lesion should be contained in a reflectance spectrum in the visible. However, the relation between the reflectance spectrum and tissue parameters such as scattering, melanin content and blood distribution is somewhat composite. This work tries to enlighten this relation in terms of a very simple analytical mathematical model, and it is demonstrated that such a model at least will contribute to a qualitative understanding of the relevance of the various parameters.

INTRODUCTION

At present, the best therapeutic technique for port-wine stains (PWS) is laser-induced selective photothermolysis. The principle is to induce thermal damage to the vessels in such a manner that the temperature of the surrounding normal dermis is maintained below the threshold for damage (1). Selectivity is obtained by choosing the proper wavelength together with a pulse duration that is equal to or smaller than the time required for heat to diffuse across the target. The wavelength is selected to correspond to a high absorption in blood together with small absorption in dermis and epidermis. The selected wavelength is usually 577 nm which corresponds to an absorption peak in oxyhaemoglobin, or 585 nm which is close to an isosbestic point in the absorption spectrum of haemoglobin and oxyhaemoglobin. The dimensions of the vessels vary over a range of 10–200 μm in diameter, but ectatic venules up to 300 μm are also found (Fig. 1). The vessels are typically located at a depth from the skin surface of 200–300 μm and deeper.

The optical penetration depth in whole blood in the wavelength region 577–585 nm is

about 30–40 μm , and the penetration depth in a typical PWS region with 5% average blood content is in the range of 100–200 μm . The pulse duration of present commercially available devices is limited to 0.45 ms, corresponding to a thermal diffusion length of about 10 μm in tissue. The depth of damage to the vessels is therefore limited by the optical penetration depth.

Fading of the intense red/purple colour of the lesions requires that the diffuse reflection coefficient in the green/yellow region ($\lambda=500\text{--}600\text{ nm}$) is increased from the typical value of 0.1–0.2 for PWS and up to the value of 0.2–0.3 for normal skin. This can be obtained if the dermal blood content is reduced to normal values for depth up to about 500–600 μm . Deeper located vessels will give rise to a faint bluish-black appearance, very much in the same manner as normal larger vessels are seen on the volar side of the extremities. A complete return to normal skin colour requires that the diffuse reflectivity in the red region ($\lambda=600\text{--}750\text{ nm}$) is brought up also to normal values, requiring that normal blood content is obtained in the upper 800–1000 μm dermal layer.

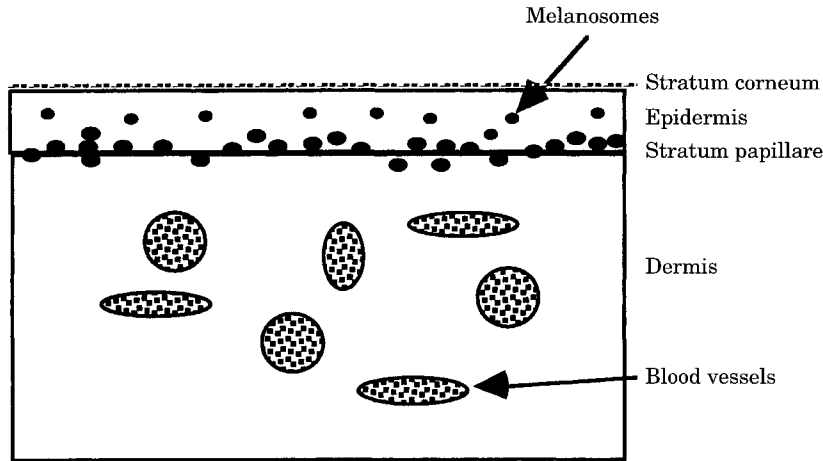


Fig. 1. Histopathology of port-wine stain.

Thin, shallow PWS lesions with thickness less than about $200\ \mu\text{m}$ might demonstrate excellent blanching after one to two treatments whereas a thick lesion might show very little improvement after the same treatment. Treatment of deep lesions might also be difficult because the optical fluence will be attenuated in the overlying normal dermis. The optical dose in normal dermis at a depth of $500\text{--}600\ \mu\text{m}$ will only be about 50–70% the dose immediately below the epidermis. However, the blanching of the PWS region is not only dependent upon reduction in blood content of the upper dermal layers; it is equally important that the scattering properties of epidermis and dermis are preserved during the treatment. The normal epidermal and dermal scattering coefficients are typically a factor of 10 larger than for muscle tissue. A reduction of this coefficient by a factor of 4–5 has the consequence that even though excessive dermal blood content is returned to normal values, the skin will still maintain the typical PWS coloration.

Overheating of the epidermis and the dermis during treatment with a subsequent necrosis and scarring will alter the scattering coefficient. Epidermal overheating is primarily due to absorption in melanin, hence a high content of melanin can be a limitation to a good therapeutic result. The possibility for epidermal overheating also increases with repeated treatments even if the irradiant dose is kept the same. The epidermal fluence in treated and blanched regions will, due to an increase in the internally backscattered light, be about 20% higher than in the untreated region.

However, it is possible to protect the epidermis from thermal damage by selectively cool-

ing it prior to laser exposure (2, 3). Selectivity is obtained by taking advantage of the dynamics of the cooling process. A sudden cooling of the skin surface will create a cold region that expands into deeper dermal layers with time. The cold region propagates into skin as a dispersive wave, and the time required to reach a certain depth is proportional to the square of the distance from the surface. The time delay before the cold front will reach the layer of the abnormal port-wine stain blood vessels at a typical depth of $2\text{--}300\ \mu\text{m}$, is of the order of 100 ms. Therefore, if the duration of the cooling is less than 50 ms, it is possible to cool the epidermis without affecting the temperature of the dermis. In treatment of deep lesions it might be necessary to increase the optical dose well above the threshold level for epidermal damage. In such cases the epidermis and the upper $300\ \mu\text{m}$ of the normal dermis can be protected from an unacceptable temperature rise by cooling for about 200 ms prior to firing the laser pulse.

A good therapeutic response might also require that the epidermis and dermis have a normal structure prior to treatment: PWS lesions with abnormal low scattering might never obtain normal coloration even if repeated treatments have restored a normal blood vessel density in the entire dermis.

The present study evaluates the influence on the visual appearance of normal skin and port-wine stains by scattering, melanin content and blood distributions. The analysis uses a simple mathematical analytical model based on optical diffusion theory. The reason for using such a simple model is that it enables an understanding for the importance of the various parameters. It should also be remembered that

any mathematical model of a complex, inhomogeneous structure, such as skin must be based on very extensive simplifications. However, even though the predicted values might only be of semi-quantitative character, they will still carry significant qualitative information.

The presented model may give a qualitative understanding that might be useful when establishing the treatment protocol.

PROPERTIES OF BLOOD AND SKIN

The optical properties of human erythrocytes at 685 nm wavelength are reported as $\mu_{sc,b} = 55.09 \times 10^{-12} \text{ m}^2$, $\mu_{ac,b} = 0.059 \times 10^{-12} \text{ m}^2$, and $g_b = 0.9949$ for, respectively, the scattering cross section, the absorption cross section and the average cosine of the scattering angle (4).

The corresponding coefficients for whole blood with haematocrit H is (5),

$$\begin{aligned} \mu_{a,b} &= \mu_{ac,b} \frac{H}{v_e} \\ \mu_{s,b} &= \mu_{sc,b} \frac{H(1-H)(1.4-H)}{v_e} \\ \mu_{s,b}^1 &= \mu_{sc,b} \frac{H(1-H)(1.4-H)}{v_e} (1-g_b) \end{aligned} \quad (1)$$

where $\mu_{a,b}$, $\mu_{s,b}$ and $\mu_{s,b}^1$ are, respectively, the absorption coefficient, the scattering coefficient and the reduced scattering coefficient. The erythrocyte volume v_e is $v_e = 1.25 \times 10^{-16} \text{ m}^3$.

The spectral dependence of the absorption coefficient for 80% oxygenated blood at physiological concentration (150 g l^{-1} haemoglobin or $H=0.41$) is shown in Fig. 2. The graph, which is based on the following empirical-analytical approximation, corresponds well with data in the literature for the visible part of the spectrum (6, 7)

$$\begin{aligned} \mu_{a,b,80} &= H \, 25 \, 000 \left(30e^{-\left(\frac{\lambda-415}{20}\right)^2} + 2e^{-\left(\frac{\lambda-450}{65}\right)^2} \right. \\ &+ 3.2e^{-\left(\frac{\lambda-545}{25}\right)^2} + 2.4e^{-\left(\frac{\lambda-577}{14}\right)^2} + 0.25e^{-\left(\frac{\lambda-590}{28}\right)^2} \\ &+ 0.035e^{-\left(\frac{\lambda-600}{90}\right)^2} + 0.01e^{-\left(\frac{\lambda-760}{10}\right)^2} + 0.075e^{-\left(\frac{\lambda-900}{215}\right)^2} \end{aligned} \quad (2)$$

The wavelength λ is in nm.

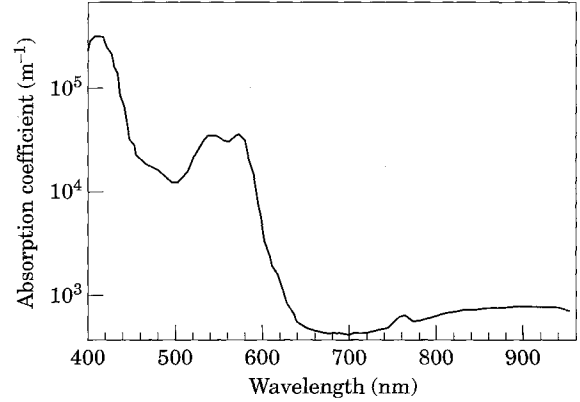


Fig. 2. Absorption coefficient versus wavelength in whole blood of haematocrit $H=0.41$ with 80% oxygenation.

The scattering coefficient of the dermis and the epidermis is reported to be strongly wavelength dependent in the ultra-violet region. The wavelength dependence is more weak in the 450–800 nm region where the coefficient is almost proportional to the inverse wavelength. The scattering coefficient has been reported to be $\mu_s = 50 \text{ mm}^{-1}$ at $\lambda = 577 \text{ nm}$ (8–10). The wavelength-dependent scattering coefficient thus becomes,

$$\mu_{s,e} \approx \mu_{s,d} = \frac{29 \times 10^6}{\lambda} \quad (3)$$

where $\mu_{s,e}$ and $\mu_{s,d}$ are, respectively, the epidermal and dermal scattering coefficients, and the wavelength, λ , is in nm. Very few reported experimental values for dermal scattering coefficients are available, but a value of $\mu_{s,d} = 21.7 \text{ mm}^{-1}$ at $\lambda = 633 \text{ nm}$ has also been reported (8).

The scattering is strongly forward directed and the average cosines of the scattering angle are reported to be in the region of $g=0.8$. The following expressions for the wavelength dependence of g is reported (8)

$$g_e \approx g_d = 0.62 + 29 \times 10^{-5} \lambda \quad (4)$$

where λ is in nm.

The scattering coefficient of the port-wine stain region will be estimated as the weighted average between the properties of blood and normal dermis. The scattering coefficient and the reduced scattering coefficients are thus expressed,

$$\begin{aligned} \mu_{s,pws} &= \mu_{s,d}(1-B_{pws}) \\ &+ \mu_{sc,b} \frac{H(1-H)(1.4-H)}{\nu_e} B_{pws} \end{aligned} \quad (5)$$

$$\begin{aligned} \mu_{s,pws}^1 &= \mu_{s,d}(1-g_d)(1-B_{pws}) \\ &+ \mu_{sc,b} \frac{H(1-H)(1.4-H)}{\nu_e} (1-g_b)B_{pws} \end{aligned}$$

The absorption coefficients of the epidermis, the normal dermis and of the port-wine stain region will correspondingly be expressed as weighted averages of melanin and blood absorption. The melanin absorption is strongly wavelength dependent and in the wavelength region 500–900 nm it is approximately proportional to the fourth power of the inverse wavelength (6). The absorption coefficients can thus be expressed,

$$\begin{aligned} \mu_{a,e} &= \mu_{a,m,694} \left(\frac{694}{\lambda} \right)^4 + \mu_{a,b} B_e + \mu_{a,n} \\ \mu_{a,d} &= \mu_{a,b} B_d + \mu_{a,n} \\ \mu_{a,pws} &= \mu_{a,b} B_{pws} + \mu_{a,n} (1-B_{pws}) \end{aligned} \quad (6)$$

In the mathematical model the epidermal/papillary dermis layer will be defined as a layer of uniform thickness containing all the melanosomes. The non-planar geometry of the stratum papillare implies that the absorption in blood in the papillae should be taken into account for this layer. The absorption coefficient of the epidermal layer, $\mu_{a,e}$, is therefore taken as the sum of the average melanin absorption ($\mu_{a,m,694}$ at 694 nm), blood absorption due to blood in the papillae (average blood fraction, B_e , in the total epidermal layer) and $\mu_{a,n}$, which is a non-melanin and non-blood related absorption in the dermis and epidermis. This last value is taken to correspond to the absorption coefficient of low absorption tissues such as the human eye and uterine tissue, i.e. typically $\mu_{a,n} = 0.025 \text{ mm}^{-1}$ at 600–900 nm (11). The absorption coefficient in the dermis, $\mu_{a,d}$, is taken as the contribution from the blood fraction, B_d , together with the same wavelength independent term as in the epidermis, e.g. the total absorption coefficient at 585 nm with a blood fraction of 1% will be $\mu_{a,d} = 0.26 \text{ mm}^{-1}$. The absorption coefficient of the port-wine stain layer, $\mu_{a,pws}$, is taken as the

weighted average of the contribution from the blood fraction, B_{pws} , and the bloodless dermis.

The average absorption coefficient of epidermal melanin was measured in vivo with irradiance from a pulsed laser. The properties were evaluated from the threshold irradiated fluence for immediate whitening of the epidermis (12). In order to avoid artefacts from absorption in haemoglobin, the measurements were done at 694 nm where skin absorption is dominated by melanin. The measurements were done with a free-running ruby laser with 0.5 ms pulse length. The thermal diffusion length in epidermis for this pulse length, i.e. $10 \mu\text{m}$, is larger than both the melanosomal dimension ($0.5\text{--}1 \mu\text{m}$) and the inter-melanosomal distance ($2\text{--}5 \mu\text{m}$), but still short compared to the epidermal thickness ($60\text{--}100 \mu\text{m}$) (3, 13). The heat will therefore be almost uniformly distributed over the epidermis, and very little heat will diffuse out of the epidermal layer during the pulse. The average epidermal absorption coefficient can therefore be found from the approximate expression (see Appendix, equations A7 and A8),

$$\mu_{a,m,694} + \mu_{a,n} = \frac{\kappa \Delta T}{\chi \Phi_{tot} \Delta \tau} = \frac{\kappa \Delta T}{\chi W_0 \left(1 + \frac{\gamma}{A} \right)} \quad (7)$$

where $\Delta T = 80 \text{ K}$ is the temperature rise required to increase the temperature from the normal value of $30 \text{ }^\circ\text{C}$ to the threshold level for thermal damage at $110 \text{ }^\circ\text{C}$ (14). The parameters Φ_{tot} , κ , χ and $\Delta \tau$ are respectively, the sub-surface fluence rate, the thermal conductivity (0.45 W mK^{-1}) (11), the thermal diffusivity ($1.1 \times 10^{-7} \text{ m}^2 \text{ s}^{-1}$) (11) and the pulse length (0.5 ms). The incident energy density is given by W_0 . The diffuse reflection coefficient is given by γ , and $\mu_{a,n}$ is the non-melanin related tissue absorption coefficient. The parameter A characterizes the internal reflection of diffuse light at the skin–air interface. This parameter is determined by the index of refraction of skin. This index of refraction decreases with water content and a maximum of $n = 1.55$ is reported for stratum corneum (11, 15). The value for A is calculated to $A = 0.17$ for an index of refraction equal to $n = 1.4$. The sub-surface fluence rate is a factor of $(1 + \gamma/A)$ larger than the incident irradiation (see Appendix, equation A13).

The measurements give values for the threshold incident fluence W_0 from 10–15 to

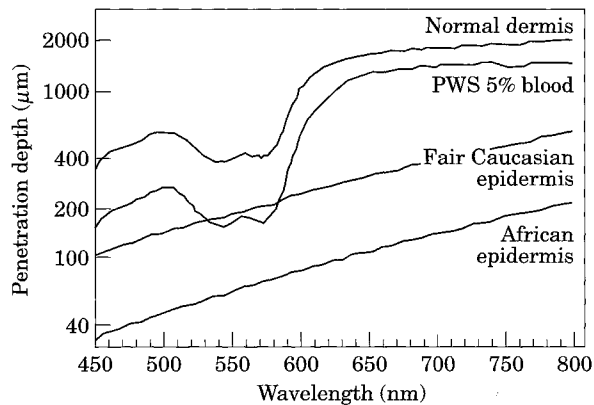


Fig. 3. Penetration depth in skin and PWS vs wavelength. Average melanin absorption coefficient: fair Caucasian $\mu_{a,m,694}=0.300 \text{ mm}^{-1}$, African $\mu_{a,m,694}=2 \text{ mm}^{-1}$. Scattering coefficient: epidermis $\mu_{s,e,577}=50 \text{ mm}^{-1}$, dermis $\mu_{s,d,577}=25 \text{ mm}^{-1}$.

$20\text{--}25 \text{ J cm}^{-2}$. The lower set of values was found for moderately dark Asian and Caucasian skin (Middle East), and the upper values are for fair Caucasian skin (North European). The diffuse reflection coefficients at 694 nm for moderately dark Asian and Caucasian skin (Middle East) were determined to be 0.42–0.48 and the corresponding values for North European skin were 0.45–0.55. These values determine an average absorption coefficient for moderately dark skin in the range of $\mu_{a,m,694}=0.535\text{--}0.905 \text{ mm}^{-1}$ and a corresponding set of values for fair skin of $\mu_{a,m,694}=0.280\text{--}0.325 \text{ mm}^{-1}$. However, no epidermal damage was observed in sun-protected North European skin for an incident fluence up to about 30 J cm^{-2} , thus indicating an average melanin absorption coefficient less than $\mu_{a,m,694}=0.225 \text{ mm}^{-1}$. The actual absorption coefficient of the individual melanosomes will, since they occupy only 0.1–1% of the epidermal volume, be two to three orders of magnitude higher than the average value.

The calculated penetration depths versus wavelengths in the epidermis, the dermis and the port-wine stain region are shown in Fig. 3. The volume fractions of blood in epidermis/papillary dermis, dermis and PWS are, respectively, 0.2%, 1% and 5%.

DISCUSSION

Measured in vivo, diffuse reflectivity for various types of normal skin is shown in Fig. 4. The spectra were measured with an integrating sphere. Spectra N.E.1 and N.E.2 were

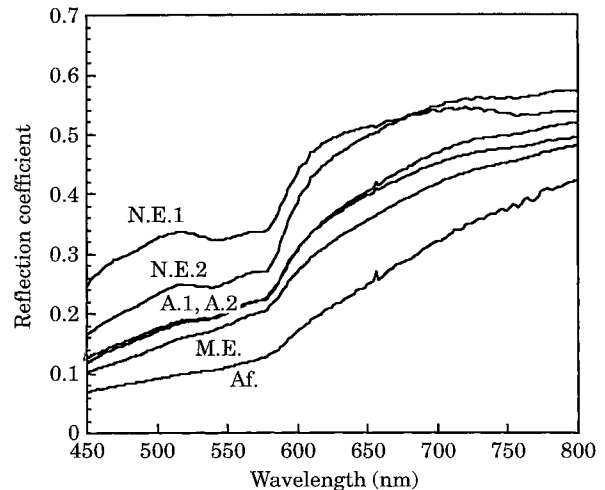


Fig. 4. In vivo diffuse reflectance spectra for human skin of various pigmentation (see text for abbreviations).

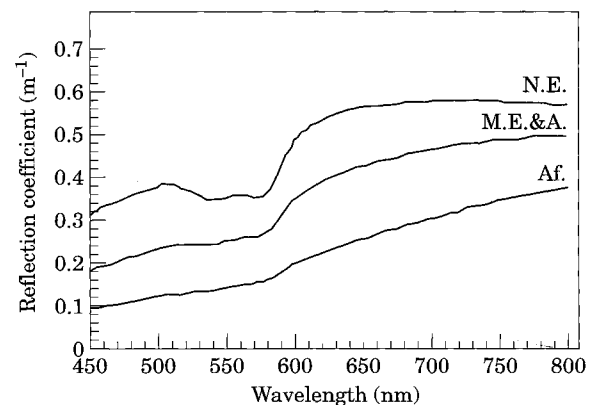


Fig. 5. Reflection coefficient of skin vs wavelength. N.E.: Fair Caucasian (North European); M.E.&A.: Caucasian (Middle East) and Asian; Af.: African.

measured on North European skin. The curve marked N.E.1 was measured on a fairly white region on the volar side of the upper arm whereas N.E.2 gives the results for the sun-tanned dorsal side of the same arm. Spectra A.1 and A.2 were taken at the dorsal side of the forearm of two Asian males having moderately pigmented skin, and curve M.E. gives values from the same region of a Caucasian male from the Middle East. The lower curve, Af., gives the corresponding spectrum for a female of African origin.

The corresponding calculated reflectance spectra are shown in Fig. 5. The calculation is based on a simple two-layer model (see Appendix, equation A14). The blood volume fractions in the epidermis/papillary layer and in the dermis are, respectively, 0.2% and 1%. The epidermal and dermal scattering coefficients are, respectively, $\mu_{s,e,577}=50 \text{ mm}^{-1}$ and

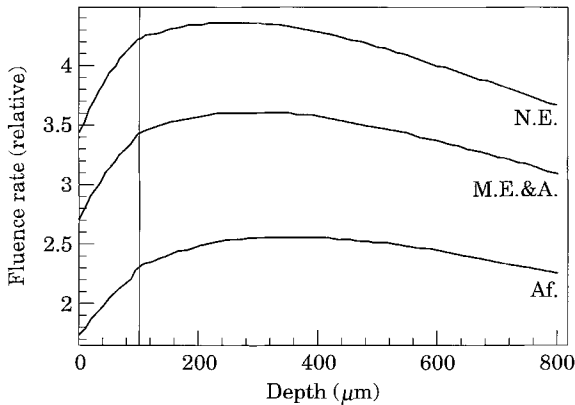


Fig. 6. Diffuse optical fluence rate versus depth in epidermis (0–100 μm) and dermis. Wavelength 694 nm. (See Fig. 5 legend.)

$\mu_{s,d,577} = 25 \text{ mm}^{-1}$. The upper curve is valid for an average melanin absorption coefficient corresponding to very fair North European skin, $\mu_{a,m,694} = 0.3 \text{ mm}^{-1}$; the middle curve corresponds to Middle East and moderately pigmented Asian skin, $\mu_{a,m,694} = 0.8 \text{ mm}^{-1}$; and the lower curve gives the reflection coefficient for African skin, $\mu_{a,m,694} = 2.0 \text{ mm}^{-1}$.

The reflection spectra of Caucasian skin clearly demonstrate the haemoglobin absorption for wavelengths shorter than 600 nm, whereas the spectrum of African skin is dominated by melanin absorption.

The correlation between the calculated spectra in Fig. 5 and the measured ones in Fig. 4 is good. However, the fact that the calculated values tend to be higher than the measured ones might indicate that the used values for the epidermal and dermal scattering coefficients are somewhat too high.

The reflection coefficient in the red–near-infrared region, which is about one order of magnitude higher than the specular reflected light, is due to the build-up of a strong diffuse fluence rate in the epidermis and upper dermis. A typical distribution for the diffuse fluence rate in this wavelength region is shown in Fig. 6, which shows the diffuse fluence rate at 694 nm wavelength for an incident collimated beam with power density normalized to unity. The diffuse fluence rate in Caucasian and Asian skin is thus about 3.5–4.5 times higher than the irradiance. The corresponding value for African skin is about 2.5. The total fluence rate, i.e. the sum of the power density in the unscattered collimated incident beam and the diffuse fluence rate, is shown in Fig. 7. The corresponding distributions for a wavelength in the yellow part of

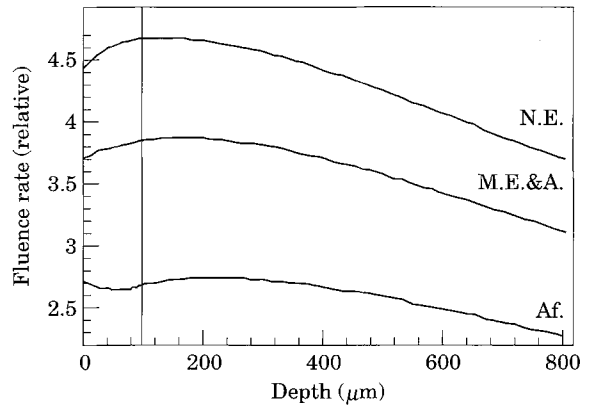


Fig. 7. Total optical fluence rate versus depth in epidermis (0–100 μm) and dermis. Wavelength 694 nm. (See Fig. 5 legend.)

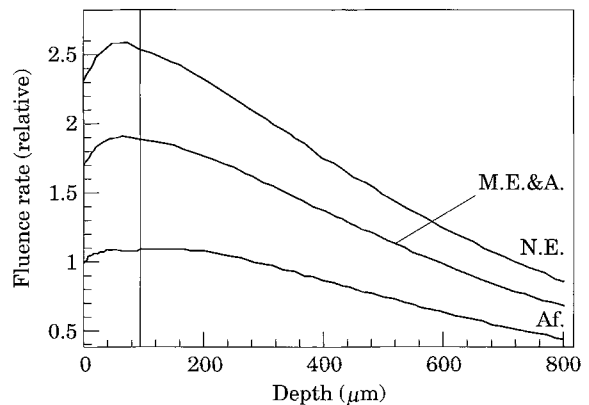


Fig. 8. Diffuse optical fluence rate versus depth in epidermis (0–100 μm) and dermis. Wavelength 585 nm. (See Fig. 5 legend.)

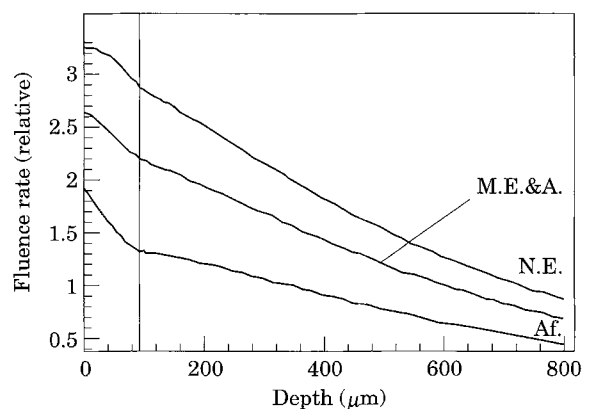


Fig. 9. Total optical fluence rate versus depth in epidermis (0–100 μm) and dermis. Wavelength 585 nm. (See Fig. 5 legend.)

the spectrum, i.e. 585 nm, are shown in Figs 8 and 9.

Calculated reflectance spectra for Caucasian skin with PWS are shown in Fig. 10. The average melanin absorption coefficient

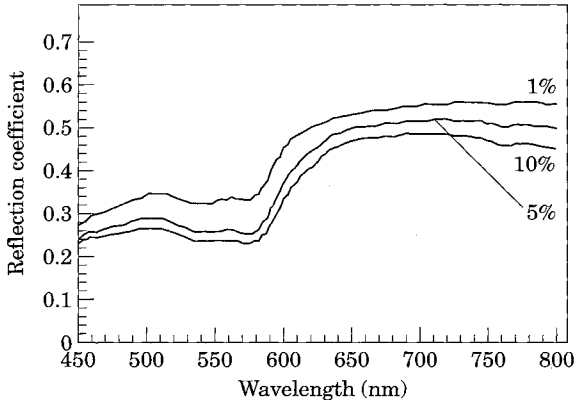


Fig. 10. Reflection coefficient of normal skin and PWS with different blood fractions (5% and 10%) vs wavelength.

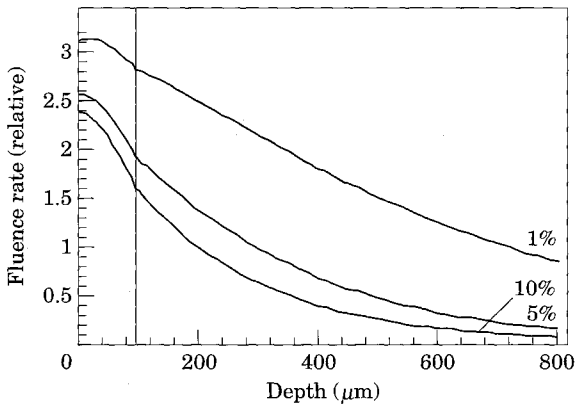


Fig. 11. Total optical fluence rate versus depth in epidermis (0–100 μm) and dermis. Wavelength 585 nm.

$\mu_{a,m,694} = 0.4 \text{ mm}^{-1}$ corresponds to moderately fair Caucasian skin. The calculation is based on the two-layer model assuming that the PWS inflicts the entire dermis (see Appendix, equation A14). The upper curve corresponds to a normal dermal blood content of 1% whereas

the middle and the lower curves correspond to, respectively, PWS with 5% and 10% blood content. The epidermal/papillary dermis blood fraction is 0.2%, and the epidermal and dermal scattering coefficients are, respectively, $\mu_{s,577} = 50 \text{ mm}^{-1}$ and $\mu_{s,577} = 25 \text{ mm}^{-1}$. A simple estimate of the redness of the skin can be found from the ratio between the reflection coefficient in the green/yellow and in the red part of the spectrum, e.g. from the ratio between the diffuse reflectances at 550 nm and 650 nm. A low value of this ratio corresponds to an intense red colour and a value equal to 1 corresponds to a complete white surface. The ratio is about 0.5 for the PWS regions shown in Fig. 10 and the ratio is about 0.6 for normal skin coloration.

The corresponding distribution of the total optical fluence in the dermis and epidermis at 585 nm wavelength is shown in Fig. 11.

High reflectivity is strongly dependent on a high scattering coefficient. An example of the effect of a lower epidermal scattering is shown in Fig. 12(a) where the epidermal scattering coefficient has been reduced by a factor of 2 compared with the value used in Fig. 10. Figure 12(b) shows the additional effect of a lower dermal scattering.

The results shown in Fig. 12(a, b) show that a reduction of the scattering coefficient by a factor of 2 has a significant impact on the reflectivity. This effect is further demonstrated in Fig. 13. The upper two curves correspond, respectively, to normal dermis with 1% blood and to a PWS with 5% blood content. The scattering coefficients have the same values as those used in Fig. 5. The lower curve corresponds, however, to a normal 1% blood content whereas the epidermal and the dermal

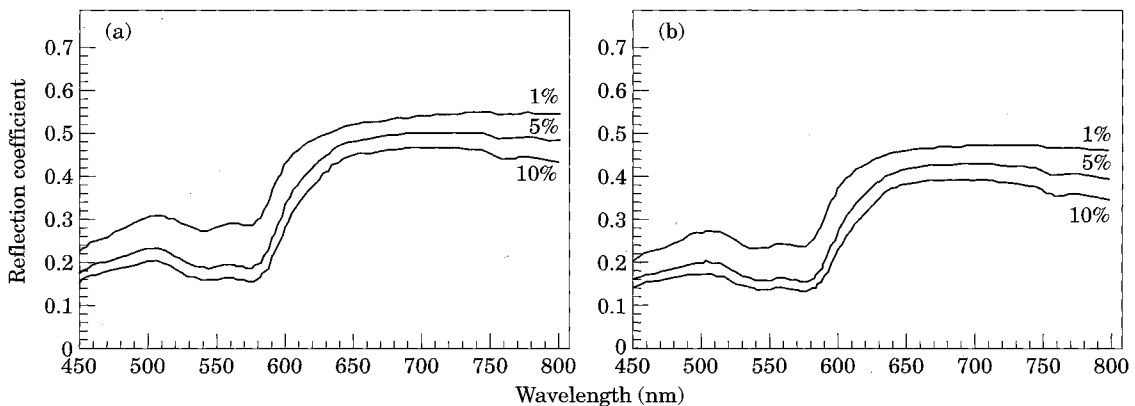


Fig. 12. Reflection coefficient of normal skin and PWS vs wavelength. (a) Scattering coefficient epidermis $\mu_{s,577} = 25 \text{ mm}^{-1}$, dermis $\mu_{s,577} = 25 \text{ mm}^{-1}$. (b) Scattering coefficient epidermis $\mu_{s,577} = 25 \text{ mm}^{-1}$, dermis $\mu_{s,577} = 12.5 \text{ mm}^{-1}$.

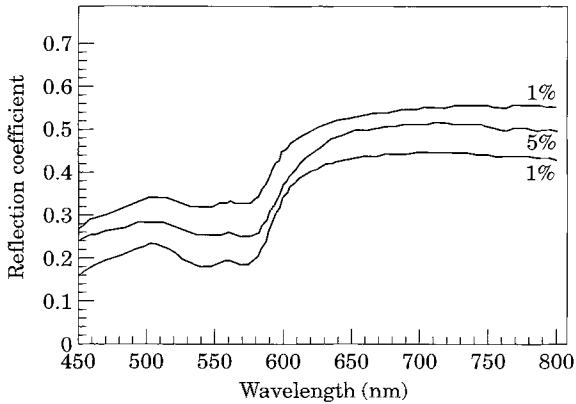


Fig. 13. Reflection coefficient of normal skin (upper curve), PWS (middle curve) and skin with normal dermal blood content but with reduced scattering (lower curve).

scattering coefficients are reduced to $\mu_{s,577} = 10 \text{ mm}^{-1}$. It should be noted that this low value is still two to three times larger than the scattering coefficients for most other tissues. The reduced scattering results in a significant reddening and darkening of normal skin.

The influence of the thickness of the PWS layer on the reflectance spectrum can be evaluated in terms of a three-layer analytical model (see Appendix, equations A7 and A8). Figure 14(a) shows variation in the reflectance at 585 nm as function of the thickness of the PWS region. The PWS layer is assumed to start at the dermal/epidermal boundary at $100 \mu\text{m}$ depth, and the thickness is varied from 0 to 1.4 mm. The reflected yellow light is reduced with increasing layer thickness up to about $150\text{--}200 \mu\text{m}$; any layer thicker than this would appear to have an infinitely large thickness.

The corresponding result for 694 nm wavelength is shown in Fig. 14(b). The reflectance here is decreasing with increasing layer thickness up to about $800\text{--}1000 \mu\text{m}$. Shallow, thin PWS lesions will therefore have a more well-defined red colour than thick lesions; the additional reduction in backscattered red light in thicker lesions will result in a more dark red/blackish colour.

The corresponding influences on the reflection coefficient from the depth of the PWS layer are shown in Fig. 15. The PWS layer is assumed to start at a variable depth from stratum papillare whereas it always extends down to the dermal/subcutaneous fat boundary region. The reflected yellow light increases with increasing depth for depths up to about $400\text{--}500 \mu\text{m}$ as shown in Fig. 15(a). The reflected red and near-infra-red light increases with increasing depth up to about $800\text{--}1000 \mu\text{m}$ [Fig. 15(b)]. Shallow PWS might therefore appear more bright red than deeper lesions. The bright red will shift towards more deep red as the depth of the lesion increases to about $400\text{--}500 \mu\text{m}$, and deeper lesions will appear more blue/blackish. This phenomenon is the same effect that gives large subcutaneous blood vessels in normal skin the blue/blackish colour.

The measured reflectance spectra of a young adult female Caucasian PWS patient is shown in Fig. 16. The upper curve in this figure gives the reflection coefficient of normal skin (suntanned upper back) and the lower curve gives the value in a region with a PWS on the upper back. The two middle curves give the spectra

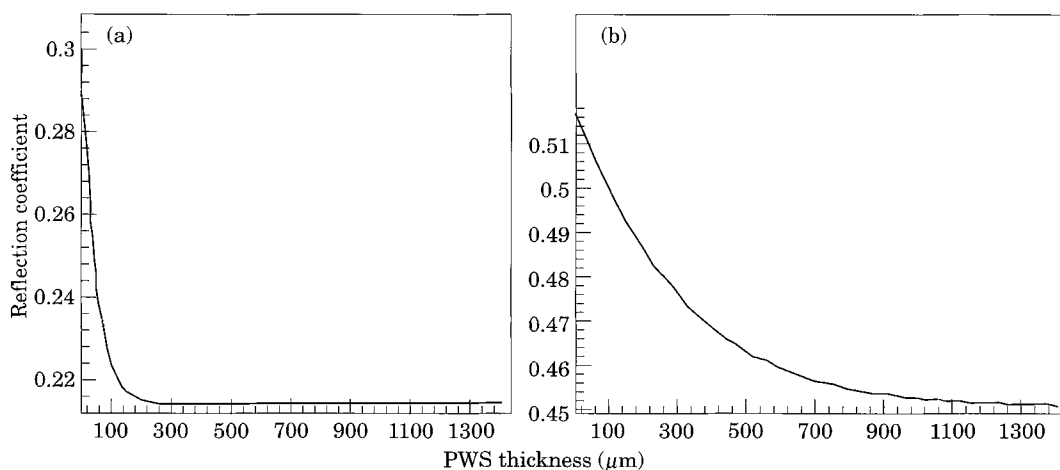


Fig. 14. Reflectance versus PWS thickness at (a) 585 nm and (b) 694 nm wavelength. Fair Caucasian skin $\mu_{a,m,694} = 0.3 \text{ mm}^{-1}$. Scattering coefficients: $\mu_{s,e} \approx \mu_{s,d} = 50 \text{ mm}^{-1}$. Blood fractions normal dermis 1.5%, PWS 15%. Epidermal thickness 0.1 mm and PWS extends from stratum papillare.

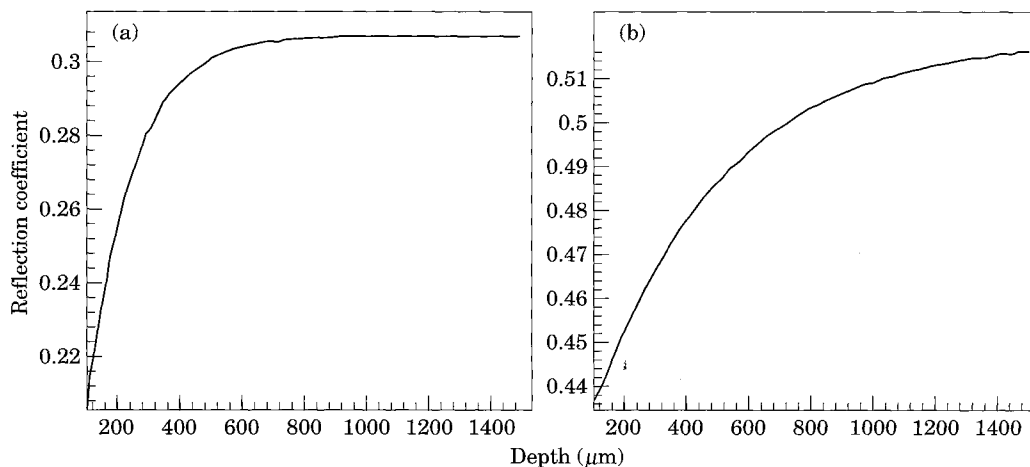


Fig. 15. Reflectance versus depth of PWS at (a) 585 nm and (b) 694 nm wavelengths.

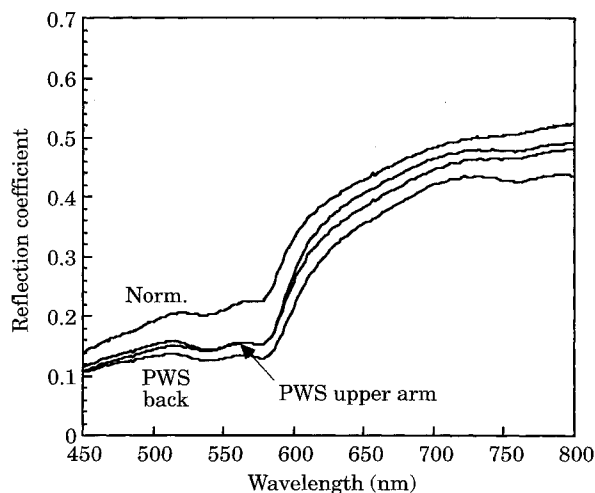


Fig. 16. In vivo reflectance spectra for normal skin and PWS of a young adult Caucasian female.

from two red/purple PWS regions on the upper arm.

CONCLUSIONS

The visual appearance of normal skin and PWS is determined by scattering, melanin content and blood volume fraction in the different layers of the skin. An efficient blanching of treated PWS requires not only that the blood vessel density in the upper dermis is reduced to normal values: it is equally important that the epidermal and dermal scattering properties are maintained.

ACKNOWLEDGEMENTS

This project was supported by research grants awarded from Biomedical Research Technology Program (R03-

RR06988), Institute of Arthritis, Musculoskeletal and Skin Diseases (1R29-AR41638-01A1 and 1R01-AR42437-01A1) at the National Institute of Health, Whitaker Foundation, Dermatology Foundation, ONR (N00014-91-0134), DOE (DE-FG-3-91ER61227), LAMP-NIH (R01192) and the Beckman Laser Institute and Medical Clinic Endowment. One of the authors (L. T. Norvang) acknowledges the support from the Norwegian Research Council.

REFERENCES

- 1 Anderson RR, Parrish JA. Selective photothermolysis: precise microsurgery by selective absorption of pulsed radiation. *Science* 1983, **220**:524-7
- 2 Nelson JS, Milner TE, Anvari B et al. Dynamic cooling during pulsed laser treatment of port wine stain—a new methodology with preliminary clinical evaluation. *Arch Dermatol* (in press)
- 3 Svaasand LO, Milner TE, Anvari B et al. Epidermal heating during laser induced photothermolysis of port wine stains: modeling melanosomal heating after dynamic cooling the skin surface. *SPIE Europto Series* 1994, **2323**:366-77
- 4 Ishimaru A. *Wave Propagation and Scattering in Random Media*. New York: Academic Press, 1978:66
- 5 Steinke JM, Shepherd AP. Diffusion model of the optical absorbance of whole blood. *J Opt Soc Am* 1988, **5**:813-22
- 6 Hillenkamp F. Interaction between laser radiation and biological systems. In: Hillenkamp F, Pratesi R, Sacci C (eds) *Lasers in Biology and Medicine*. New York: Plenum Press, 1979:57, 61
- 7 van Gemert MJC, Welch AJ. Clinical use of laser-tissue interactions. *IEEE Eng Med Biol Magazine* 1989, **8**(4):10-3
- 8 van Gemert MJC, Jacques SL, Sterenborg HJCM, Star WM. Skin optics. *IEEE Trans Biomed Eng* 1989, **36**:1146-54
- 9 Wan S, Anderson RR, Parrish JA. Analytical modeling for the optical properties of the skin in vitro and in vivo applications. *Photochem Photobiol* 1981, **34**:493-9
- 10 Anderson RR, Parrish JA. Optical properties of human skin. In: Regan JD, Parrish JA (eds) *The Science of Photomedicine*. New York: Plenum Press, 1982:147-194

- 11 Duck FA. *Physical Properties of Tissue*. London: Academic Press, 1990
- 12 Hruza GJ, Dover JS, Flotte TJ et al. Q-switched ruby laser irradiation of normal human skin. *Arch Dermatol* 1991, **127**:1799–805
- 13 Moschella SL, Hurley HJ. *Dermatology*, 3rd edn. London: W. B. Saunders, 1992:1421–35
- 14 Jacques SL, McAuliffe DJ. The melanosome: threshold temperature for explosive vaporization and internal absorption coefficient during laser irradiation. *Photochem Photobiol* 1991, **6**:769–75
- 15 Scheuplein RJ. A survey of some fundamental aspects of the absorption and reflection of light by tissue. *J Soc Cos Chem* 1964, **15**:11–122
- 16 Haskell RC, Svaasand LO, Tsay T-T et al. Boundary conditions for the diffusion equation in radiative transfer. *J Opt Soc Am* 1994, **11**:2727–41

Key words: Port-wine stains; Reflection spectra; Scattering coefficients; Absorption coefficients; Optical diffusion

APPENDIX

The analysis uses a simple mathematical analytical model based on the optical diffusion theory. Although the validity of the diffusion theory is limited in thin regions such as the epidermal layer, the precision of the calculated values for the reflection coefficient is good. The reason for this is that the reflected light has contributions not only from very superficial regions but also from deeper dermal layers. The diffusion approximation assumes an almost isotropic light distribution and radiance L can be expressed by a series expansion of the form (4, 16)

$$L = \frac{\phi}{4\pi} + \frac{3}{4\pi} \vec{j} \cdot \vec{l} + \dots \quad (\text{A1})$$

where ϕ and \vec{j} are, respectively, the fluence rate and the diffuse photon flux vector. The first term in this series expansion corresponds to an isotropic radiance and the second term represents the deviation from isotropy in the direction given by the unit directional vector \vec{l} .

The irradiance on a surface normal to the flux then becomes,

$$E = \frac{\phi}{4} \pm \frac{j}{2} \quad (\text{A2})$$

where the + and – signs are valid for, respectively, a surface facing against the flux and along the flux. The diffuse photon flux vector \vec{j} is given by,

$$\vec{j} = -\zeta \text{grad} \phi \quad (\text{A3})$$

The diffusion constant is given by $\zeta = 1/3\mu_{tr} = 1/3(\mu_s(1-g) + \mu_a)$ where μ_{tr} , μ_s , g and μ_a are, respectively, the transport coefficient, the scattering coefficient, the average cosine of the scattering angle and the absorption coefficient.

The steady-state equation of continuity can be expressed,

$$\text{div} \vec{j} = -\mu_a \phi + q \quad (\text{A4})$$

where q is the source density of diffuse photons. These two equations can be combined to yield,

$$\nabla^2 \phi - \frac{\phi}{\delta^2} = -\frac{q}{\zeta} \quad (\text{A5})$$

where $\delta = \sqrt{1/3\mu_{tr}\mu_a}$ is the optical penetration depth.

The boundary conditions between two scattering media can be expressed by the continuity of irradiance in the forward and backward directions, i.e.

$$\begin{aligned} \frac{\phi_1}{4} + \frac{j_1}{2} &= \frac{\phi_2}{4} + \frac{j_2}{2} \\ \frac{\phi_1}{4} - \frac{j_1}{2} &= \frac{\phi_2}{4} - \frac{j_2}{2} \end{aligned} \quad (\text{A6})$$

This equation can also be expressed in terms of continuity of the fluence rate together with continuity of the flux.

A very useful boundary condition at the skin–air interface is obtained by relating the reflected part of the irradiation at the inside of the interface to the irradiation propagating back into the skin (16)

$$R_{eff} \left(\frac{\phi}{4} + \frac{j}{2} \right) = \frac{\phi}{4} - \frac{j}{2} \quad (\text{A7})$$

where R_{eff} is the effective reflection coefficient. The value of R_{eff} that can be found by integrating the Fresnel reflection coefficient for unpolarized light over all angles of incidence is 0.431 and 0.493 for respectively an index of refraction of $n=1.33$ and $n=1.40$.

This condition can also be expressed in the form,

$$j = A\phi \quad (\text{A8})$$

where $A = (1 - R_{eff})/2(1 + R_{eff})$. The basic criterion of optical diffusion theory that the flux shall be much smaller than the fluence rate is thus only satisfied to a limited degree at the surface

where $A=0.2-0.17$ for $n=1.33-1.4$ (16). However, the ratio is small enough to justify the use of the diffusion theory as a reasonably good approximation.

A three-layer model of the skin is composed of an epidermal layer extending to depth d_1 , a normal dermis extending from d_1 to d_2 and a PWS layer extending from depth d_2 to infinity. The depth of the epidermal layer is taken to the deepest region of the stratum papillare. This definition implies that the epidermal/stratum papillare layer will contain the blood in the papillae in addition to all the melanin.

The incident light density P first undergoes specular reflection at the skin-air interface and the transmitted light P_0 is assumed to be gradually scattered to an isotropic distribution. The source density of diffuse photons in the layers will thus be expressed,

$$\begin{aligned} 0 < x < d_1 \\ q_1 &= P_0 \mu_{s,1}^1 e^{-\mu_{r,1}x} \\ d_1 < x < d_2 \\ q_2 &= P_0 \mu_{s,2}^1 e^{-\mu_{r,1}d_1} e^{-\mu_{r,2}(x-d_1)} \\ d_2 < x < \infty \\ q_3 &= P_0 \mu_{s,3}^1 e^{-\mu_{r,1}d_1} e^{-\mu_{r,2}(d_2-d_1)} e^{-\mu_{r,3}(x-d_2)} \end{aligned} \quad (\text{A9})$$

where x is the distance from the skin surface and $\mu_s^1 = \mu_s(1-g)$ is the reduced scattering coefficient. The indices 1, 2 and 3 refer, respectively, to the epidermis, the normal dermis and the dermis with PWS.

The solutions in the different regions can thus be written,

$$\begin{aligned} \varphi_1 &= \frac{P_0 \delta_1^2 \mu_{s,1}^1}{\zeta_1 (1 - \mu_{r,1}^2 \delta_1^2)} e^{-\mu_{r,1}x} + A_1 e^{-\frac{x}{\delta_1}} + A_2 e^{\frac{x}{\delta_1}} \\ \varphi_2 &= \frac{P_0 \delta_2^2 \mu_{s,2}^1}{\zeta_2 (1 - \mu_{r,2}^2 \delta_2^2)} e^{-\mu_{r,1}d_1} e^{-\mu_{r,2}(x-d_1)} + A_3 e^{-\frac{x}{\delta_2}} + A_4 e^{\frac{x}{\delta_2}} \\ \varphi_3 &= \frac{P_0 \delta_3^2 \mu_{s,3}^1}{\zeta_3 (1 - \mu_{r,3}^2 \delta_3^2)} e^{-\mu_{r,1}d_1} e^{-\mu_{r,2}(d_2-d_1)} e^{-\mu_{r,3}(x-d_2)} \\ &+ A_5 e^{-\frac{x}{\delta_3}} \end{aligned} \quad (\text{A10})$$

The values for the constants A_1-A_5 can be found by using the boundary condition given in equation A8 at the skin-air interface together with the conditions of continuity of

fluence rate and flux at the epidermis-dermis boundary and at the normal dermis-PWS dermis boundary (equation A6). The diffuse reflection coefficient from the skin can then be expressed by,

$$\gamma = \frac{j|_{x=0}}{P_0} \quad (\text{A11})$$

which follows from equations A3 and A10.

The diffuse fluence rate in the upper epidermal layer, ie the stratum corneum, can be expressed,

$$\varphi|_{x=0} = \frac{j|_{x=0}}{A} = \frac{2(1+R_{eff})}{1-R_{eff}} \gamma P_0 \quad (\text{A12})$$

When taking the unscattered incident flux into account, the total subsurface fluence rate, φ_{tot} , thus becomes,

$$\varphi_{tot} = \varphi|_{x=0} + P_0 = \left(\frac{2(1+R_{eff})}{1-R_{eff}} \gamma + 1 \right) P_0 \quad (\text{A13})$$

The expression for the reflection coefficient in the three-layer model is of very simple mathematical structure. However, it is somewhat composite and will therefore not be written out in detail. The reflection coefficient of the two-layer model follows from equations A3, A10 and A11,

$$\begin{aligned} \gamma &= \delta_1 \mu_{s,1}^1 A \left\{ \left[\left(\frac{\delta_1^2 \delta_2}{3} - \delta_1^2 \zeta_2 \right) \cosh \left(\frac{d_1}{\delta_1} \right) \right. \right. \\ &+ \left. \left(\frac{\delta_1^3 \zeta_2}{3 \zeta_1} - \delta_1 \delta_2 \zeta_1 \right) \sinh \left(\frac{d_1}{\delta_1} \right) \right] \left(1 + \frac{\delta_2}{3 \zeta_2} \right) \right. \\ &+ \left. \left[\frac{\mu_{s,2}^1}{\mu_{s,1}^1} \delta_2^2 \zeta_1 \left(\frac{\delta_1^2}{9 \zeta_1^2} - 1 \right) + \delta_1^2 \left(\zeta_2 - \frac{\delta_2^2}{9 \zeta_2} \right) \right] e^{-\frac{d_1}{3 \zeta_1}} \right\} \\ &\left\{ \left(\frac{\delta_1^2}{9 \zeta_1^2} - 1 \right) \left(\frac{\delta_2}{3 \zeta_2} + 1 \right) \left[\zeta_1 \delta_1 (\zeta_2 + \delta_2 A) \cosh \left(\frac{d_1}{\delta_1} \right) \right. \right. \right. \\ &+ \left. \left. \left. (\zeta_1^2 \delta_2 + \zeta_2 \delta_1^2 A) \sinh \left(\frac{d_1}{\delta_1} \right) \right] \right\}^{-1} \end{aligned} \quad (\text{A14})$$

The spectra shown in Figs 3 and 5-8 are calculated from this equation whereas the values in Figs 9 and 10 are found from the three-layer model given in equation A9.